Motion of injected charges in hcp ^{4}He crystals

A. I. Golov, V. B. Efimov, and L. P. Mezhov-Deglin

Institute of Solid-State Physics, Academy of Sciences of the USSR, Chernogolovka, Moscow Province

(Submitted 24 April 1987)
Zh. Eksp. Teor. Fiz. **94**, 198–218 (February 1988)

The velocities of positive and negative charges in hcp ^{4}He crystals were measured at temperatures $T > 0.5$ K. The range of working pressures was $P = 25.5$–40 atm, the applied fields were $E = 3\times10^3$–1.3×10^5 V/cm, and the velocities varied from $v = 5\times10^5$ to 1×10^{-1} cm/s. The velocity of positive charges $v_+(T)$ in weak fields $E \leqslant 10^4$ V/cm had a maximum as a function of temperature at $T = 0.7$–0.9 K and the $v_+(E)$ curves describing the field dependence of the velocity in strong electric fields in $E \geqslant 5\times10^4$ V/cm also had a maximum at temperatures below 0.9 K. In the same fields the drift velocity of negative charges v_- rose monotonically with the field. The difference between the temperature and field dependences of the velocities v_+ and v_- was evidence of a difference between the mechanisms of transport of positive and negative charges in hcp ^{4}He crystals.

1. INTRODUCTION

A.I. Shal'nikov formulated the problem of the properties of injected charges in a solid which act as microscopic probe particles in the lattice of a quantum crystal and move across this crystal under the influence of an applied electric field. The first successful experiments on charges in solid helium were carried out in his laboratory.[1–8] The steady-state properties of a diode with a radioactive charge source in solid helium were investigated first and this was followed by direct measurements of the charge velocity by a transit-time method in a triode (when a control grid was inserted between the source and collector). The most detailed investigation of the behavior of the mobility of charges in the range of thermally activated motion in ^{4}He was carried out by Keshishev.[7,8]

These measurements stimulated a number of theoretical and experimental investigations of the properties of charges in solid helium (see, for example, the reviews of Andreev[9] and Shikin[10]). A similar analysis of the work published up to 1985 with numerous references was made in the review by Dahm.[11] The present paper reports a continuation of the experimental studies begun earlier[12] and it describes measurements of the velocity of charges in hcp ^{4}He crystals carried out in a wide range of fields and temperatures. As in Ref. 12, the average velocity of the charges was determined from the time of arrival of a front of charged particles at a diode collector subjected to a step-like voltage. A comparison of the results obtained with those reported in Refs. 7 and 8 demonstrated that where the working ranges of fields and temperatures overlapped, the results of transit-time measurements of the velocity in a diode and triode were practically identical. New results were obtained in ranges not investigated thoroughly before, i.e., at temperatures below 0.9 K and in fields in excess of 5×10^4 V/cm. The most interesting of the new results were as follows.

1) Maxima were found in the temperature dependences $v_+(T)$ of the velocity of positive charges in weak electric fields $E \leqslant 1\times10^4$ V/cm at the same temperatures (below 0.9 K) where maxima of the temperature dependences of the steady-state current $I_+(T)$ were reported in Ref. 12.

2) The positive charge velocity v_+ was above a certain threshold field $E \geqslant 5\times10^4$ V/cm.

3) The negative charge velocity v_- increased monotonically with the field, in contrast to the positive charges. In strong fields $E \geqslant 5\times10^4$ V/cm the dependence $v_-(E)$ was nearly exponential.

Some of the results of the preliminary measurements in samples grown under a pressure of $P \approx 31$ atm were reported in brief communications.[13,14] Since the thermometers were recalibrated in the course of the main measurements, the temperature dependence of the velocity $v_+(T)$ obtained below 0.7 K reproduced in Fig. 1 in the present paper is somewhat steeper than that shown in Fig. 1 in Ref. 13. The results of measurements of the charge mobility in hcp and bcc ^{4}He samples characterized by similar molar volumes were reported in Ref. 15.

2. EXPERIMENTAL METHOD

Our measurements were made using the same apparatus as in Ref. 12. Helium crystals were grown under a constant pressure ($\Delta P/P \leqslant 1.5\%$) in a cylindrical ampoule 7.5 mm in diameter and 60 mm long. Two thermometers and two heaters placed outside along the edges of an ampoule made it possible to monitor the distribution of the temperature along a sample. The ampoule was cooled with a copper heat sink connected to a bath containing liquid ^{3}He.

The thermometers were calibrated against the vapor pressure of liquid ^{4}He and ^{3}He. A comparison of the calibration of the thermometers placed at the ampoule with the calibration of the same thermometers inside a ^{3}He bath showed that the ampoule containing solid helium was at a somewhat higher temperature than the ^{3}He bath because of the evolution of heat by two β-active charge sources located inside the ampoule and because some heat reached the ampoule along the measuring circuits. Above 1 K this temperature difference was unimportant, but when the sample was cooled to 0.5 K the difference between the calibrations increased to hundredths of a degree Kelvin because of an increase in the Kapitza thermal resistance at the helium–copper interface, which was ignored in an analysis of the thermometer calibration in preliminary experiments.[13,14]

The ampoule contained two planar diodes consisting of identical β-active sources (titanium–tritium targets on molybdenum substrates) and molybdenum collectors of

 0038-5646/88/020325-11$04.00

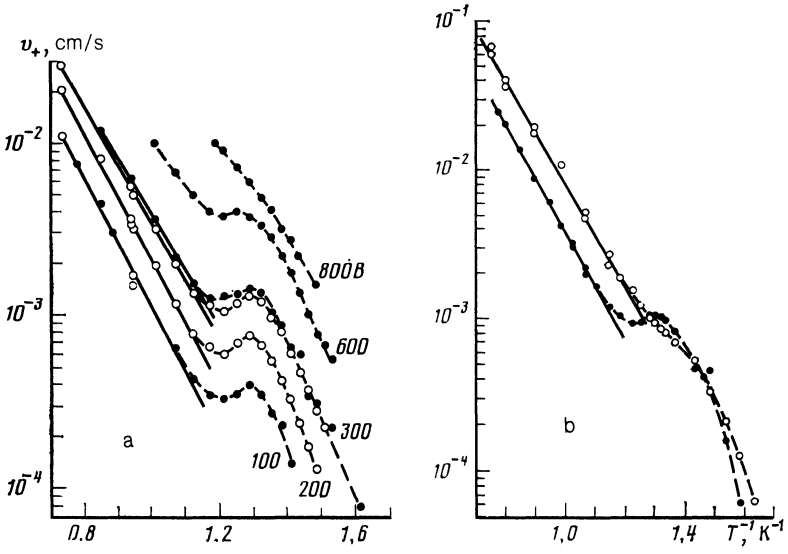

FIG. 1. Temperature dependences of the positive charge velocity in four samples grown at $P = 31 \pm 0.2$ atm: a) samples 116 (31.2 atm) denoted by O and 117 (31.0 atm) denoted by ●; b) samples 149 (30.8 atm) denoted by O and 149A (30.8 atm) denoted by ●. The applied voltage was $U = 300$ V.

$36\times6\times0.5$ mm dimensions. The distances between the diode electrodes were $L = 1.0$ and 0.3 mm. Since the transit-time measurements required too much time in the wide diode at low temperatures, all the results reported below were obtained for the diode with $L = 0.3$ mm.

The characteristics of the diodes were known[7,16]: the average energy of the emitted β particles was 5.7 keV, the maximum energy was ≈ 18 keV, the range of β particles in condensed helium was up to 10 μm. On the average, each particle created about 200 ion pairs in helium, so that a layer of positively charged helium ions was formed near the target (these ions were He_n^+ complexes with $n\geqslant 1$—see Ref. 11) surrounded by a region of compressed helium and a layer of negatively charged particles (electrons) was localized in helium at pressures below 40 atm in a cavity of $R_- \approx 10^{-7}$ cm radius.[10,11] The sign of the charges moving across a crystal was governed by the polarity of the applied voltage U. The saturation currents in the targets in helium were $I_{sat} = 2\times10^{-8}$ A, but in contrast to Ref. 3, all the measurements in the present study were carried out using currents $I \ll I_{sat}$.

In addition to β particles, the target emitted weak electromagnetic radiation.[16] Oppositely directed constant currents in the grid–collector gap due to the emission of photoelectrons from the collector made it difficult to carry out transit-time measurements in weak fields in a triode[7,8] at low temperatures. In our experiments the influence of weak opposed currents on the results of transit-type measurements in a diode was unimportant, since the positive charge velocity v_+ in all the samples was much higher than the negative charge velocity v_- throughout the investigated range of temperatures and fields.

The transit time τ, representing the time taken to cross the source–collector base by a front of moving particles as a result of application of a voltage step U, was deduced from the positions of the maxima of the $I(t)$ curves representing the time dependence of the collector current. This method of determining the velocity of injected charges from the transient characteristics of a diode had been known for a long time.[17] Calculations of the shape of the $I(t)$ curves on the assumption that the velocity depends linearly on the field were made in Refs. 18 and 19.

In the case of an infinitely high charge density at the source the collector current is limited by the space charge and the charge front travels in an inhomogeneous electric field, so that the time of arrival τ of the front at the collector is 1.27 times smaller than the transit time τ^* for the crossing of the source–collector base by a solitary charge moving in a homogeneous field $E = U/L$. In practically all our measurements the collector current was $I \leqslant I_{sat}$, i.e., we were operating in the space-charge-limited (SCL) regime. Therefore, the velocity $v(U)$ deduced from the arrival time of the front in a sample subjected to a given potential U was related to the velocity of a single charge $v^*(E)$ in a weak homogeneous field E by

$$v(U) \equiv L/\tau = 1.27 v^*(E). \qquad (1)$$

The linear field dependences reported in Refs. 7, 8, 12, and 18 were observed in our study but only in weak fields $E \leqslant 1\times10^4$ V/cm. When the field satisfied $E \geqslant 2\times10^4$ V/cm, dependences $v^*(E)$ faster and slower than linear were obtained. Clearly Eq. (1) was not obeyed in the case of the nonlinear dependence $v^*(E)$. Calculations of the time of arrival of a front at the collector were made in Ref. 20 for the SCL range assuming a power-law dependence $v^*(E) \propto E^n$, where $n \geqslant 1$. The values of the ratio τ^*/τ for $n = 1, 2, 3, 5, 7$, and 10 were 1.27, 1.37, 1.45, 1.47, 1.51, and 1.52, respectively.

In all the experiments in which the velocity rose monotonically with the field, the maximum values of the power exponent were $n \leqslant 5$. When n was increased from 1 to 5 the ratio τ^*/τ rose by at least a factor of 1.2. Therefore, in estimating the power exponent n from the experimental $v(U)$ curves we could, in the first approximation, assume that

$$v^*(E) = v(U)/(1.4\pm0.1), \qquad (2)$$

i.e., $v^*(E) \propto v(U) \propto U^n$, if the relative width of the range of fields in which this estimate was obtained amounted to $\Delta U/U \geqslant 1$.

It was more difficult to reconstruct the form of the $v^*(E)$ curve in the case of a nonmonotonic field dependence of the velocity, for example, when the velocity $v(U)$ fell at voltages above a certain critical value (which was true of

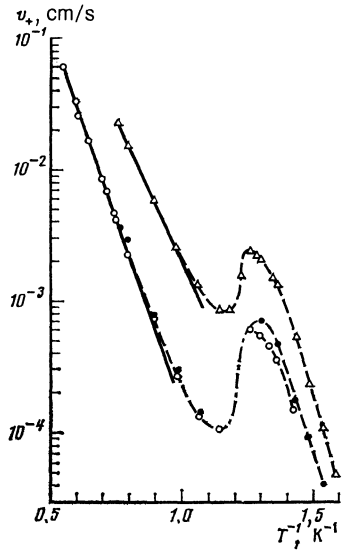

FIG. 2. Dependence $v_+(T)$ obtained for three different samples grown at pressures in excess of 32 atm: △) sample 130 (33.3 atm); ○) sample 171 (35.6 atm); ●) sample 172 (35.9 atm). $U = 300$ V.

positive charges in strong fields). A numerical calculation of the inverse problem [in which a given dependence $v^*(E)$ was used to calculate the form of the $v(U)$ curve] given in the Appendix demonstrated that the $v^*(E)$ and $v(U)$ curves were qualitatively similar, although the positions of maxima on the original and "experimental" curves, and their relative amplitudes, could differ.

Special experiments and calculations[11,12,18–20] demonstrated that the capture of charges by defects in the interior of a sample had little influence on the front arrival time τ, but reduced considerably the static current (in the $t \gg \tau$ case) compared with the current at the maximum of $I(\tau)$. Consequently, the results of measurements of dynamic and static characteristics of a diode in weak fields at temperatures above 1 K could be used to judge the quality of the samples and to select those with fewer defects for detailed investigation. Some of the sample had $I(t)$ curves with two or three maxima, which clearly represented motion at different velocities in large blocks of different orientation (the hcp crystals are highly anisotropic) or they exhibited quasiperiodic oscillations of the static current and the frequency of these oscillations varied with temperature (such oscillations were reported also by Dahm,[11] who attributed their appearance to the motion of dislocation walls). As a rule, all such defective samples were melted and replaced with new samples.

The results reported below were obtained for samples for which the $I(t)$ curves had one clear maximum, the current at the maximum was of the order of the static value, and the results of transit-time measurements were readily reproducible in the course of thermal cycling.

3. RESULTS OF MEASUREMENTS

3.1. Velocity of charges in weak fields

Following Eqs. (1) and (2), we shall define weak fields as those in which systematic deviations of the field dependence of the velocity $v(U)$ from linearity were less than 20%. For the majority of these samples the voltage dependence of the velocity was linear in the range $U \leqslant 300$ V, i.e., in fields $E \leqslant 1 \times 10^4$ V/cm. An increase in the pressure from 25.5 to 40 atm or cooling reduced the permissible range of values of the field on the average by a factor of 2–3.

We shall begin by reporting the results of measurements of the velocity of positive charges $v_+(T)$ in four samples grown at a pressure of $P = 31 \pm 0.2$ atm (samples 116 and 117 in Fig. 1a and samples 149 and 149A in Fig. 1b), which were grown one after the other at the same pressure. The dashed curves join the experimental points. The continuous straight lines correspond to the exponential dependence $v_+(T) \propto \exp(\varepsilon_+/T)$. The numbers alongside the curves in Fig. 1a give the values of the voltage U. We can see that at $U = 300$ V the values and temperature dependences of the velocity v_+ could differ considerably from sample to sample. For example, in the case of thirteen samples grown under a pressure of $P = 31 \pm 0.5$ atm we found that for six of the samples the values of v_+ at $T = 1$ K agreed to within $\pm 10\%$, whereas for three samples the velocities differed from these values by $\pm 20\%$ and for four samples they differed by a factor of 2–5. Clearly, this was due to the anisotropy of hcp crystals, since imperfections of the samples had little influence on the results of our transit-time measurements.

Three regions could be distinguished in the $v_+(T)$

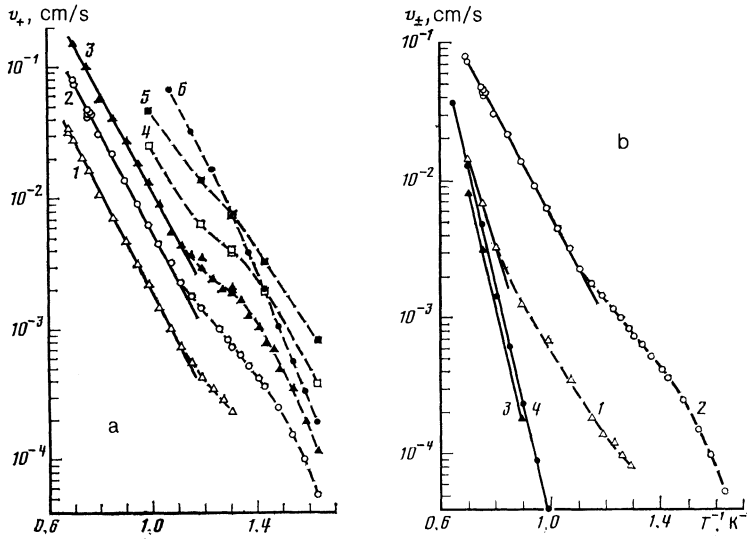

FIG. 3. Temperature dependence of the velocity of positive and negative charges in samples grown at low pressures $P < 30$ atm. a) Positive charges, sample 159 (28.8 atm). The lines join the points obtained at the same voltage: 1) U = 100 V; 2) 300 V; 3) 600 V; 4) 1.0 kV; 5) 1.6 kV; 6) 2.8 kV. b) Positive and negative charges at $U = 300$ V: 1), 2) $v_+(T)$; 3), 4) $v_-(T)$. Sample 157 (28.5 atm) is represented by curves 1 and 3 and sample 159 (28.8 atm) is represented by curves 2 and 4.

curves: a high-temperature region corresponding to $T \geqslant 1$ K and usually described by an exponential dependence, a transition region $0.9 \geqslant T \geqslant 0.7$ K, and a low-temperature region $T < 0.7$ K, where the velocity again fell strongly as a result of cooling.

The shape of the $v_+(T)$ curves in the transition region depended strongly on the solidification pressure. The curves plotted in Fig. 1 were obtained for samples grown at pressures near $P = 31$ atm. At higher pressures $P \geqslant 32$ atm it was found for all the investigated samples that in the transition region there were only maxima and at lower pressures of $P < 30$ atm there were only inflections, as shown in Fig. 1b. The corresponding examples are plotted in Fig. 2 (samples 130, 171, and 172 grown at pressures of 33.3, 35.6, and 35.9 atm) and in Fig. 3 (sample 159 grown at $P = 28.8$ atm in Fig. 3a and sample 157 grown at 28.5 atm in Fig. 3b).

At pressures above 30 atm an increase in the pressure increased the slope of the straight lines $\log v_+ = f(1/T)$ in the thermally activated diffusion region (i.e., an increase in the pressure increased the activation energy ε_+) and this was accompanied by a simultaneous increase also in the relative amplitude of the maxima in the transition region. However, when the relative amplitude of the maxima exceeded 3, we were unable to follow the evolution of the $v_+(T)$ curves near the velocity maximum when temperature was varied, because the transition characteristics $I_+(t)$ became indistinct, although outside this narrow temperature range there were still maxima in the $I_+(t)$ curves right down to the lowest temperatures. The problems were probably due to the presence of a temperature gradient along the ampoule, which was unimportant in the case of a smoother dependence $v_+(T)$.

At pressures above 37 atm the charge velocity v_+ in the linear region was far too low for a systematic investigation of the temperature dependences in weak fields below 1 K. However, at a voltage of $U = 1$ kV we were able to observe a fivefold increase in the velocity v_+ in the transition region in a crystal grown at 40 atm.

Curves 1–6 in Fig. 3a illustrated changes in the temperature dependences of the velocity $v_+(T)$ accompanied by a transition from weak to strong fields (curve 1 was obtained for a voltage of $U = 100$ V and curve 6 was obtained for $U = 2.8$ kV). The dependence $v_+(U)$ was nearly linear right up to $U = 600$ V. On the other hand, at low pressures there was a strong increase in the scatter of the values of the velocity $v_-(T)$ from sample to sample at the same growth pressure, i.e., crystals became more anisotropic. This is illustrated in Fig. 3b for samples 189 and 157 grown at pressures of $P = 28.8$ and 28.5 atm and subjected to a voltage of $U = 300$ V. We shall show later that such samples exhibited equally significant variation in the field dependence of the velocity $v_+(U)$ in strong fields.

The temperature dependence of the negative charge velocity $v_-(T)$ in the same samples at a voltage $U = 300$ V are plotted in Fig. 3b. In contrast to v_+, the values of v_- obtained in the thermally activated motion region were similar for the same pressures and depended in the same way on the external field in strong fields. Since at pressures $P < 40$ atm the velocity of negative charges was less than that of positive charges, we were unable to investigate the temperature dependence $v_-(T)$ in weak fields below 1 K.

3.2 Positive charges in strong fields

It was reported in Refs. 7 and 8 that $v_+^*(E)$ grew faster than linearly in samples grown at pressures of $P = 32.4$ and 40.5 atm, while $v_+^*(E)$ was slower than linear for a sample grown at 25.5 atm. A considerable widening of the range of working fields and temperatures showed that below 0.9 K $v_+(U)$ and, consequently, $v_+^*(E)$ were more complex and sometimes nonmonotonic in stronger fields.

We were able to identify two forms of $v_+(U)$ (Fig. 4): a) curves with a maximum; b) curves with an inflection (curves in which the derivative only decreased) in a field above a certain threshold. The dependences of the type represented by curve a in Fig. 4 were observed for all the samples grown at pressures in excess of 30 atm and for some of the samples grown at lower pressures; the dependences of the type represented by curve b in Fig. 4 were obtained only for some of the samples grown at pressures below 30 atm.

The influence of temperature on the shape of the $v_+(U)$ curves of samples of the first type is shown in Figs. 5a and 5b (samples 107 and 159). At temperatures above 0.9 K the velocity v_+ in these samples rose monotonically with the voltage. Unfortunately, the range of the field dependence $v_+(U)$ studied was limited in the thermally activated region to voltages $U \leqslant 2.2$ kV. The maximum values of U were limited, firstly, by the slow response of the recording apparatus (the time resolution was down to 0.3 s, i.e., velocities could be measured in the range $v \leqslant 1 \times 10^{-1}$ cm/s), and, secondly by strong local overheating of a sample in the course of the measurements (the current rose rapidly and thermal conductivity fell exponentially on increase in temperature). Below 1 K it was possible to carry out measurements right up to $U = 4$ kV.

Typical time dependences of a diode recorded at $T < 0.9$ K at voltages near the threshold of $U = 1.6$ kV are plotted in Fig. 6. An increase in the voltage from 1.6 to 2.4 kV shifted the maximum to the right, i.e., the arrival time of the front increased and the velocity fell. The form of the $I_+(t)$ curves was similar to the calculated curves plotted in Fig. 13 for a given dependence $v_+^*(E)$.

The field dependence of the velocity obtained in strong fields near the point of a maximum increased in steepness as a result of cooling (Figs. 5a and 5b). There was a corre-

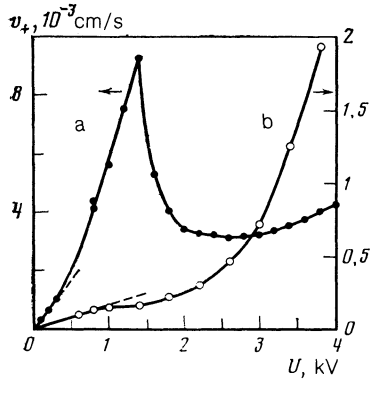

FIG. 4. Two types of field dependence of the velocity of positive charges $v_+(U)$ in strong fields. The curves are drawn through the experimental points: ●) sample 107 ($P = 30.8$ atm), $T = 0.72$ K; ○) sample 157 (28.5 atm), $T = 0.73$ K. The dashed lines are the linear dependences.

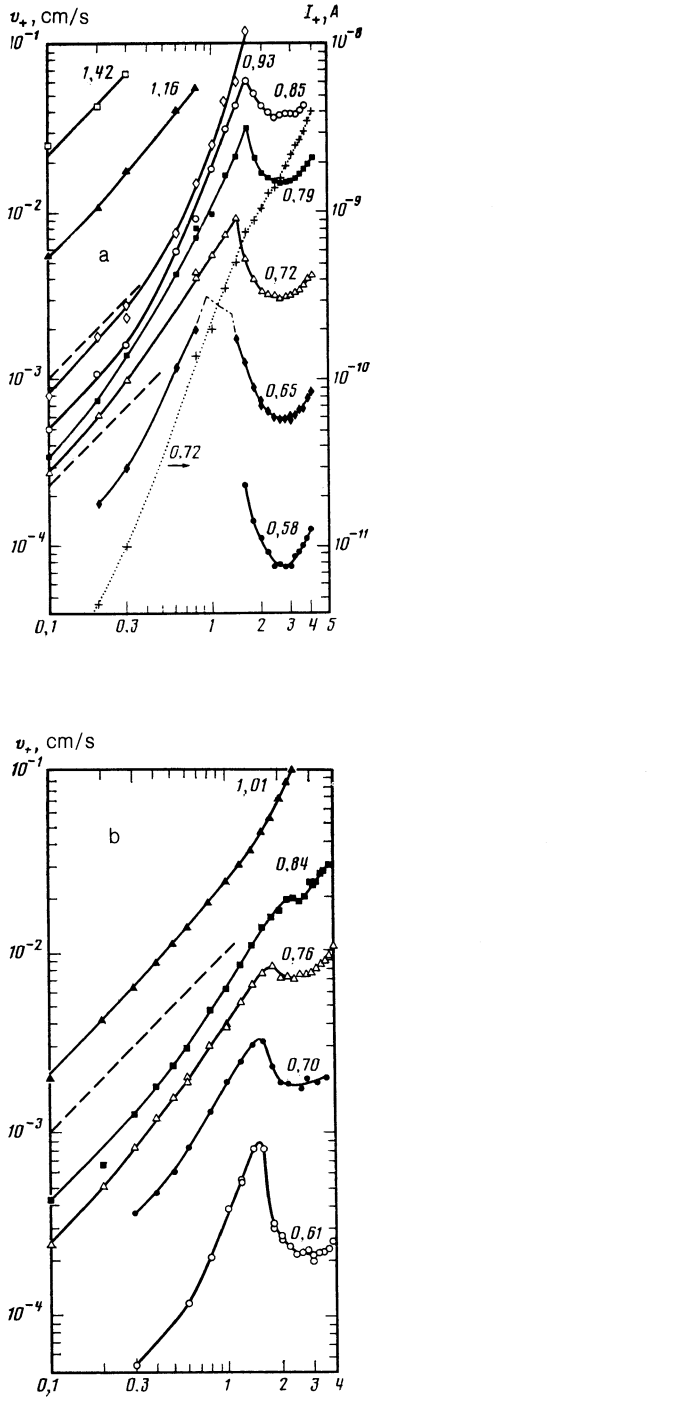

FIG. 5. Evolution of the $v_+(U)$ curves in strong fields on increase in temperature (the numbers alongside the curves give the temperatures T in degrees Kelvin): a) sample 107 (30.8 atm); b) sample 159 (28.8 atm); c) sample 157 (28.5 atm). The dashed lines represent the linear dependences $v_+(U)$. The crosses represent the dependence of the steady-state current $I_+(U)$ at $T = 0.72$ K in sample 107.

sponding increase in the relative amplitude of the maxima. In fields above the threshold the velocity v_+ reached its minimum at $U = 2.8$ kV ($E \approx 9 \times 10^4$ V/cm) and then increased strongly again. In the region of the maximum the value of v_+ decreased as a result of cooling in accordance with the nearly exponential law (sample 159, curve 6 in Fig. 3a; sample 107 was similar to sample 117 shown in Fig. 1a).

The crosses in Fig. 5a represent the field dependence of the steady-state current $I_+(U)$ at $T = 0.72$ K (in Fig. 1 of Ref. 14 the first two points of the same dependence were shifted incorrectly by an order of magnitude in the upward direction). The kink of the $v_+(U)$ curve was manifested only by a change in the slope of the $I_+(U)$ curve, which was the current-voltage characteristic of a diode in strong fields. This was in agreement with the calculated dependences $I_+(U)$ given in the Appendix.

Field dependence of the type shown in Fig. 4b was obtained only for those samples which were grown at low pressures $P < 30$ atm and which were distinguished by a low velocity v_+ in weak fields (sample 157 in Fig. 5c, for which the data were plotted also in Figs. 4b and 3b). In contrast to the samples with a dependence of the type shown in Fig. 4a, inflections of the $v_+(U)$ curves were observed both below and above 0.9 K, i.e., the shape of the $v_+(U)$ curves in fields near the threshold was independent of temperature and the threshold voltages were considerably less than for samples

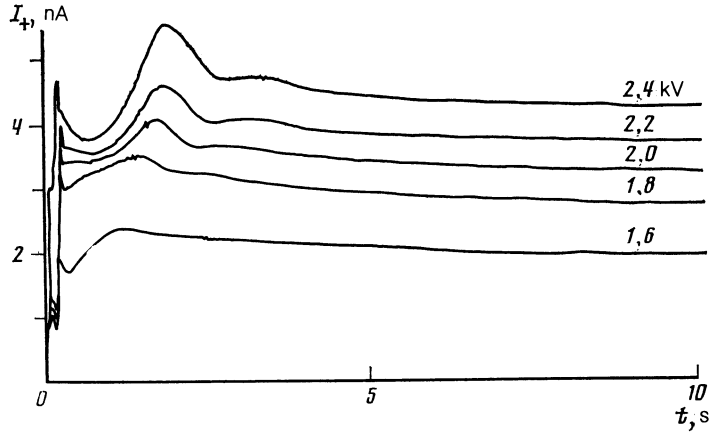

FIG. 6. Samples of the time dependence of the current $I_+(t)$ obtained applying voltages above the threshold value to sample 107 at $T = 0.79$ K.

with curves of the type shown in Fig. 4a. At all temperatures $v_+(U)$ was nearly linear to the left of the inflection, whereas it varied more slowly to the right of the inflection, but this became faster than linear in fields $E \geqslant 7\times10^4$ V/cm similar to those shown in samples of type 4a. Since the quality of the samples had practically no influence on the arrival time of the front, significant differences in the field dependences of the velocity $v_+(U)$ in samples grown at pressures close to the minimum value necessary for solidification could be explained only by the strong anisotropy of the properties of these quantum crystals.

3.3. Negative charges in strong fields

The field dependence of the negative charge velocity in strong fields was investigated in less detail than that of the positive charge velocities. In all the measurements the velocity v_- rose monotonically with pressure. Figure 7 gives the field dependence $v_-(U)$ obtained for sample 107 at different temperatures (given alongside the curves). The dashed curves represent the power laws $v_-(U) \propto U^n$, where $n = 1$, 3, or 5. Clearly, at $T = 0.85$ K in fields $U \geqslant 2.5$ keV ($E \geqslant 8\times10^4$ V/cm) the field dependence was close to $v_-(U) \propto U^5$. In the experiments described in Refs. 7 and 8 only a near-cubic dependence $v^*_-(E)$ was observed in strong fields, since measurements were limited to weaker fields ($E \leqslant 6\times10^4$ V/cm) and higher temperatures.

The field and temperature dependences of the charge velocity in bcc ^{3}He crystals obtained in Refs. 12 and 20 were described by single relationships of the Arrhenius type:

$$v(T, U) = A \exp(-\varepsilon/T)\operatorname{sh}(\gamma U/T), \qquad (3)$$

where A, ε, and γ are parameters calculated numerically for all the experimental points. We attempted to analyze similarly the results of measurements of $v_-(T,U)$. The dependences of the ratio $v_-/A\exp(-\varepsilon/T)$ on the reduced voltage U/T for samples 107 and 157 are plotted in Fig. 8. The different symbols used in Fig. 8 represent measurements carried out at different temperatures. The continuous curves are the functions $\sinh(\gamma U/T)$. The dashed curves are the power laws $v_-(U) \propto U^n$. The values of the parameters are as follows: $A = 8.7\times10^2$ cm/s and $\varepsilon_- = 15.5$ K in Fig. 8a; $A = 1.4\times10^4$ cm/s and $\varepsilon_- = 19.2$ K in Fig. 8b. Instead of γ it is more convenient to introduce a parameter b with the dimensions of length and related to γ by

$$\gamma U/T = eEb/kT, \quad E = U/L$$

(k is the Boltzmann constant and e is the electron charge), i.e., by $b = \gamma Lk/e$. The continuous curves in Figs. 8a and 8b correspond to $b = 0.4\times10^{-8}$ and 0.5×10^{-8} cm, respectively.

We can see from Fig. 8 that the experimental points obtained at different temperatures were shifted somewhat relative to the continuous curve, i.e., strictly speaking, the value of γ could depend on temperature. Since we did not know the behavior of the velocity v_- in weak fields at temperatures below 1 K and the range of measurements above 1 K was limited to fields $U \leqslant 2.1$ kV ($E \leqslant 7\times10^4$ V/cm), the available data were insufficient to determine the dependence $\gamma(T)$ and to decide whether the relationship (3) was valid quantitatively in a wide range of fields and temperatures both above and below 1 K. One of the possible results of these measurements was that in strong fields at temperatures below 1 K the velocity v_- rose exponentially rather than in accordance with a power law when the field was increased (straight lines in strong fields plotted in Fig. 8 correspond to exponential functions) right up to fields $E = 1.3\times10^5$ V/cm.

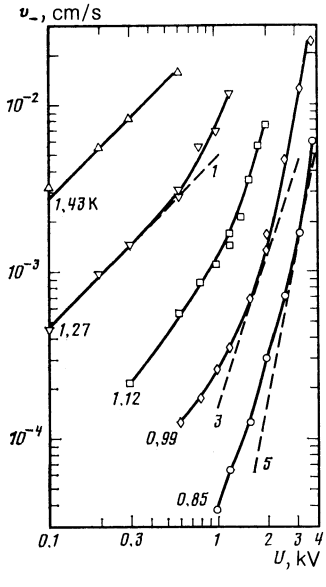

FIG. 7. Field dependence $v_-(U)$ obtained at different temperatures. The dashed lines represent the power law $v \propto U^n$, where $n = 1$, 3, or 5. Sample 107 (same as in Fig. 5a).

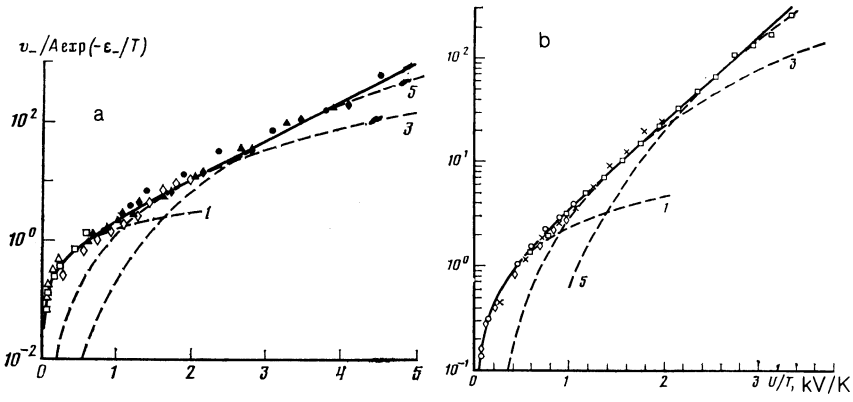

FIG. 8. Dependence of the ratio $v_-/A\exp(-\varepsilon_-/T)$ on the reduced voltage U/T applied to samples 107 (a) and 157 (b) at different temperatures (K): a)●—0.848, ◆—0.933, △—0.985, ◇1.117, □—1.351, △—1.435; b) ◇—1.43, ○—1.33, ×—1.11, □—1.22. The continuous curves represent $\sinh(\gamma U/T)$ and the dashed curves represent $v \propto U^n$ where $n = 1$, 3, or 5.

4. DISCUSSION

4.1. Positive and negative charges in weak fields observed in the range of thermally activated motion

The charge transport mechanisms in the thermally activated region are usually judged[9-11] comparing the diffusion coefficients and characteristic activation energies of the charges (D_+, ε_+) and of the He impurity atoms in samples of ^{4}He of the same molar volume (D_3, ε_3). The values of $D_\pm$ can be deduced from the charge mobility $\mu_\pm$ using the Einstein relationship

$$D_\pm = \mu_\pm kT/e. \tag{4}$$

Substituting $\mu_\pm = v^*/E = 0.8 v_\pm L/U$ in Eq. (4), we find that at a voltage $U = 300$ V and over a distance $L = 3\times 10^{-2}$ cm the diffusion coefficient is given by

$$D_\pm[\mathrm{cm^2/s}] = 0.7\cdot 10^{-8} v_\pm(300)\, T \tag{5}$$

where the velocity is measured in centimeters per second and the temperature is measured in degrees Kelvin, i.e., the transit-time method makes it possible to measure the diffusion coefficient of charges in the range $D_\pm \geqslant 10^{-13}$ cm^2/s.

The values of the ratio D_+/T are shown to the right of the ordinate in the summary graph in Fig. 9, which gives temperature dependence of the velocity $v_+(T)$ at $U = 300$ V for four typical samples grown under pressures of 38.9 atm (sample 172), 34.0 (sample 186), 31.3 (sample 184), and 28.8 (sample 159). The continuous lines in Fig. 9 represent the exponential dependences $v_+ \propto \exp(-\varepsilon_+/T)$. We can readily show that the characteristic activation energies, deduced from the slopes of such D lines, are 1–2 K less than the values occurring in expressions of the form $D = D_0 \exp(-\varepsilon/T)$, which are used to describe thermally activated diffusion of defects.

The similarity of the values of D_+ and D_3 and of the characteristic activation energies of positive charges ε_+, impurity atoms ε_3 (Ref. 21), and of vacancies ε_v (Ref. 22) has been used as the basis of vacancy models of charge transport. For example, various types of hopping are discussed in detail in Refs. 9–11: it is assumed that the motion of charges involves jumps of a charged point defect to a neighboring site of the crystal lattice at the moment when this site becomes vacant.

The results of measurements are analyzed in Refs. 7 and 8 on the assumption that vacancies in hcp ^{4}He crystals are delocalized (vacancions) and the motion of charges represents inelastic scattering of vacancions, characterized by a wavelength much shorter than the interatomic distance, by a defect of atomic size. Hence, the value of v_+ in weak fields can be used to estimate the cross section for the scattering of vacancions by charges and the field dependences can be used to find the width Δ_v of the energy band of vacancions (Δ_v is found to be of the order of several degrees Kelvin). However, the region of validity of this model and of the regime in the band motion of vacancions in ^{4}He takes place have not yet been determined. Moreover, the structure of a positive charge moving in solid helium is not yet clear: it may be an He^+ ion, an He_2^+ or He_3^+ complex (the He_3^+ complexes are stable in a gas[11]), or—as in liquid—an ice particle with a characteristic radius twice the interatomic spacing and with the structure different from the structure of the surrounding crystal lattice.

The large difference between the mobilities and activation energies of charges of different signs in hcp ^{4}He crystals at low pressures can be explained on the basis of the Shikin theory[10] by the difference between the structure of charges

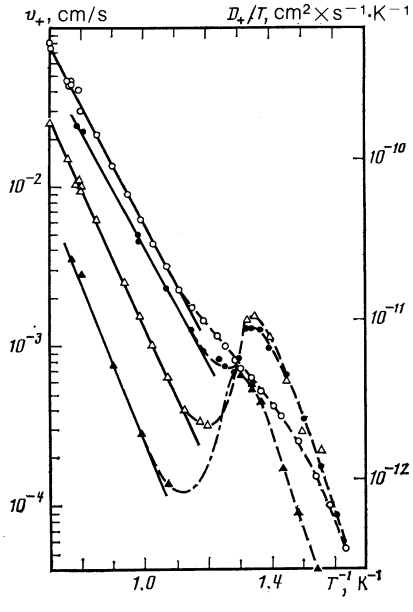

FIG. 9. Typical temperature dependence of the velocity $v_+(T)$ at $U = 300$ V obtained for samples formed at different pressures: ○) sample 159 (28.8 atm); ●) sample 184 (31.3 atm); △) 186 (33.0 atm); ▲) sample 172 (35.9 atm). The values of the ratio D_+/T are given on the right.

and the associated difference between the concentrations of thermal vacancies in the region of electrostrictive compression around charges in a crystal. The mechanism of viscoelastic flow of a crystal in the course of motion of a negative bubble of radius $R_- \approx 10^{-7}$ cm, formed around an electron in condensed helium is discussed in detail in Ref. 10. However, according to Dahm,[11] the mechanisms of motion of charges of opposite signs are fundamentally different: negative charges travel as a result of diffusion of adatoms on the internal surface of a cavity and not due to diffusion of vacancies, as is true of positive charges.

It thus follows that although the experimental results of different authors are in good agreement, the mechanisms of charge transport in hcp ^{4}He crystals in weak fields have not yet been finally established even in the thermally activated motion region. In future theoretical investigations it is necessary to allow for the fact that the ratio of the mobilities of charges of different signs changes considerably as a result of hcp–bcc phase transitions,[11,15] although the structure of the charges clearly remains the same, i.e., the structure of the crystal lattice plays an important role. For example, in the case of hcp ^{4}He formed at pressures $P < 36$ atm, we have $\mu_+ > \mu_-$ and $\varepsilon_+ < \varepsilon_-$ (at $P = 26$ atm we find that $\varepsilon_- = 22 \pm 2$ K and $\varepsilon_+ = \epsilon_v = 9 \pm 1$ K—see Ref. 22), whereas in bcc ^{4}He we find that $\mu_+ < \mu_-$ and $\varepsilon_+ > \varepsilon_-$ and in bcc ^{3}He at low pressures ($P \leqslant 50$ atm), we have $\varepsilon_+ > \varepsilon_- = \varepsilon_v$, whereas in the pressure range of $P \geqslant 60$ atm both ε_+ and ε_- are almost twice as large as ε_v for bcc crystals or for hcp phases.[12,20,22]

4.2. Positive charges in weak fields at temperatures below 0.9 K

Inflections of the $v_+(T)$ or $D_+(T)$ curves may be related to: a) a change in the properties of vacancies or a change in the nature of the interaction of charges with vacancies; b) a change in the charge transport mechanism. We shall discuss these two possibilities separately.

a) It is assumed that the charge velocity is controlled in the final analysis by the interaction with vacancies, i.e.,

$$v_+ \propto n_v D_v \sigma_v, \tag{6}$$

where $n_v \propto \exp(\varepsilon_v/T)$ is the concentration of thermal vacancies and D_v is the diffusion coefficient of vacancies, the two quantities together governing the density of the vacancy flux interacting with the moving charges; σ_v is the effective cross section for the scattering or the probability of a jump of a charge to a neighboring vacant site. Since n_v falls monotonically as a result of cooling, maxima of the $v_+(T)$ curves are observed only in the case of sharp kinks of the dependences $D_v(T)$ or $\sigma_v(T)$ because, for example, a change in vacancy diffusion mechanism or manifestation of resonant interaction of positive defects with vacancies. In both cases in a narrow range of temperatures near 0.9 K the values of D_v or σ_v should rise exponentially faster than $[n_v(T)]^{-1}$ and below the maximum they should depend weakly on temperature.

b) It is more natural to assume that kinks are related to a change in the transport mechanisms, for example, a transition from thermally activated diffusion to intrinsic subbarrier tunneling of charged defects in a quantum crystal.[23,24] Assuming that the contributions of different diffusion mechanisms are additive, we shall write down

$$D_+ = D_1 + D_2, \tag{7}$$

where $D_1 \propto \exp(-\varepsilon_+/T)$ describes thermally activated diffusion. The dependence of the coefficient $D_2(T)$ calculated on the basis of Fig. 9 is shown in Fig. 10. Cooling increases the value of D_2, which produces a maximum at $T_m = 0.8$ K and then falls strongly.

In principle, a bell-shaped temperature dependence of the diffusion coefficient of defects moving in a quantum crystal under the influence of an external force can be obtained using the results of calculations of Refs. 23 and 24. The order of magnitude of the diffusion coefficient of defects is

$$D_2[\mathrm{cm}^2/\mathrm{s}] = \frac{a^2 \Delta_+^2 \Omega_p}{3z(\Omega_p^2 + \delta^2)} \frac{k}{\hbar}. \tag{8}$$

Here, Δ_+ is the width of the energy band of a defect; Ω_p is the dynamic shift of the levels of a defect at two neighboring sites in the crystal lattice because of its interaction with phonons; δ is the static shift of the levels due to the interaction of charges with defects of different type, such as dislocations formed as a result of cooling of a sample between electrodes of a diode below $T_{mp}/2$ (Refs. 12 and 20) or due to the application of an external force field; a is the interatomic distance; z is the number of nearest neighbors in the lattice; k and $\hbar$ are the Boltzmann and Planck constants. All the energies in Eq. (8) in degrees Kelvin. The interaction of moving charges with one another can be ignored compared with an external field since the density of moving charges near a collector, estimated from the known static current and the velocity, is low ($n_\pm \sim 10^{10}$ cm^{-3} in a field $E \sim 10^4$ V/cm). Since in weak fields the coefficient D_2 (or, more exactly, the diffusion coefficient D_+) is independent of the external field, it is reasonable to assume that the static shift of the levels because of the interaction of charges with defects exceeds the shifts of the levels in an external field.

Clearly, the quantity $\Omega_p(T)$ decreases rapidly as a result of cooling. Therefore, at "high" temperatures $T > T_m$, where $\Omega_p > \delta$, the coefficient D_2 rises: $D_2 \propto 1/\Omega_p$; at "low" temperatures $T < T_m$, where $\Omega_p < \delta$, the diffusion coefficient falls in accordance with $D_2 \propto \Omega_p(T)/\delta^2$. At the maximum $T = T_m$ we have $\Omega_p(T_m) = \delta$ and hence the known value $D_2(T_m) \approx 10^{-11}$ cm/sec can be used to find typical energies Δ_+, Ω_p, and δ as soon as we know one of them. Substituting $\Omega_p(T)$ in Eq. (8), which represents the impuriton–phonon interaction, we find from Refs. 21 and 24 that $\Delta_+ = 10^{-6}$ K (which is much less than the width of the impuriton band Δ_3

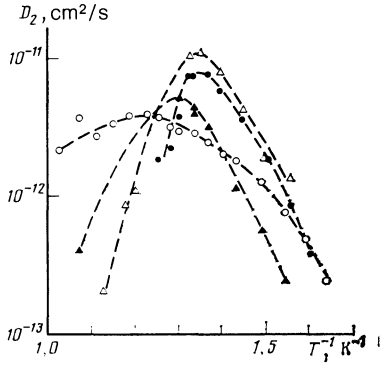

FIG. 10. Dependence $D_2(T)$. The notation is the same as in Fig. 9.

$\approx 10^{-4}$ K for crystals of the same molar volume).

Equation (8) is derived in Ref. 23 on the assumption that $T \gg \Delta_+ \gg \Omega_p, \delta$. In actual experiments the energy acquired in the course of a charge jump along the field by a distance equal to the atomic spacing exceeds 1 K. This is the reason why it is concluded in Ref. 23 that quantum diffusion of charges cannot be observed. However, it was shown in Ref. 24 that in the case of quantum diffusion of neutral defects in irregular crystals Eq. (8) is valid in a wider range: $T > \Omega_p$, $\delta > \Delta_+$, when because of the random shift of the levels a defect is practically localized at a site and it tunnels only rarely to a neighboring site. The binding energy between defects and charges captured by traps in hcp ^{4}He is of the order of 1 K (Refs. 12, 18, and 20). The exact value of δ is unimportant, since $\Delta_+ \propto \delta^{1/2}$ and we are interested only in order-of-magnitude estimates. Substituting in Eq. (8) the specific value $\Omega_p(T_m) = \delta = T_m = 0.8$ K, we obtain $\Delta_+ \approx 10^{-3}$ K which is an order of magnitude greater than Δ_3. If this estimate is valid, then the effective mass of a charged defect is less than the mass of an impuriton and the hole mechanism of charge transport may predominate (when an electron jumps from a neutral atom to an ion). This possibility was pointed out in the first papers of Shal'nikov.[1]

4.3. Strong-field dependences of the velocity of positive charges

The evolution of the shape of the curves $v_+(U)$ as a result of cooling is demonstrated in Figs. 7 and 8. Above 1 K the field dependence of the velocity of charges in samples represented by curve a in Fig. 4 is similar to the field dependence of the negative charge velocity. Therefore, an analysis of the field dependence in the region of thermally activated motion will be considered in the next section. Below 0.9 K in samples which exhibit behavior like that represented by curve a in Fig. 4 the shape of the $v_+(U)$ curves changes drastically in strong fields. A summary of the dependences in Fig. 11 includes $v_+(U)$ curves for seven different samples of the type represented in Fig. 4a (curves 1–6) and 4b (curves 7 and 8) at $T = 0.72 \pm 0.01$ K. The continuous curves are drawn through the experimental points and the dashed lines show the region of the linear dependence $v_+(U)$. Curves 1–4 correspond to the most frequently encountered behavior: 1) sample 189 (34.0 atm); 2) sample 184 (31.3 atm); 3) sample 107 (30.8 atm); 4) sample 156A (29.1 atm). Curves 5 and 6 represent sample 156 grown under the same conditions as sample 156A, but its time dependence exhibited two clear maxima, i.e., this sample consisted of two large blocks with different orientations. Curves 7 and 8 describe the $v_+(U)$ dependence obtained for samples 157 (28.5 atm) and 109 (26.2 atm).

The summary graph in Fig. 11 shows clearly a correlation between the mobility of charges in weak fields and the shape of the $v_+(U)$ curves in strong fields. In the thermally activated region at pressures in excess of 30 atm the activation energies ε increased and the charge mobilities μ fell on the average monotonically as the pressure increased. Below 20 atm the value of ε_+ depended weakly on P and the scatter of the mobilities from sample to sample reached an order of magnitude, indicating an increase in the anisotropy of the properties of hcp crystals on approach to the minimum solidification pressure. Below 0.9 K an increase in the pressure increased on the average the mobility μ_+ in samples of the

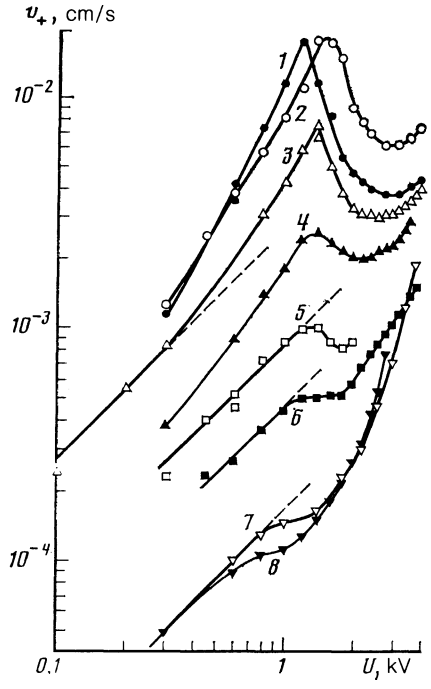

FIG. 11. Field dependence of the velocity $v_+(U)$ at $T = 0.72 \pm 0.01$ K obtained for seven samples: 1) sample 189 (34.0 atm); 2) sample 184 (31.3 atm); 3) sample 107 (30.8 atm); 4) sample 156A (29.1 atm); 5), 6) sample 156 (29.1 atm); 7) sample 157 (28.5 atm); 8) sample 109 (26.2 atm). The curves are drawn through the experimental points. The dashed lines represent the linear dependence.

type shown in Fig. 4a, in contrast to the thermally activated diffusion region. At the same time there was a reduction in the range where the dependence was linear and the relative amplitude of the maxima of curves 1–6 increased. Samples of the type shown in Fig. 4b exhibited a minimum mobility at low temperatures and the threshold voltages at which inflections appeared in curves 5 and 8 were half the values for samples of the type shown in Fig. 4a.

It seemed of interest to account for the maxima of the $D_+(T)$ and $v_+(T)$ curves exhibited by samples of the type shown in Fig. 4a by a unified sub-barrier mechanism of tunneling of positive charges [in expressions such as Eq. (8) the velocity of charges in an external field falls with increasing field if $\delta(E) > \Omega_p$]. However, this would require further development of the theory of transport of injected charges in quantum crystals.

There is also a different and more intuitive model.[14] The fall of the velocity of v_+ in fields above a certain threshold may be attributed to creation of dislocation loops capable of capturing charges and moving together with them across a crystal, in the same way quantum vortex rings appear around charges in a superfluid liquid. As in a liquid, the fall of the velocity of a charged complex with increasing field may be explained by an increase in the loop radius. The possibility that changes could form dislocations in solid helium was first pointed out by Nosanov and Titus.[25] Experiments on the motion of a frozen-in sphere in solid ^{4}He (Ref. 26) and a study of the processes of recovery in bent crystals[27] indicated that the mobility of freshly formed dislocations in helium is very high and depends exponentially on temperature with an activation energy close to ε_v. This is in agree-

ment with the temperature dependence of the velocity v_+ observed at a voltage $U = 2.8$ kV, which corresponds to the position of the minimum of the $v_+(U)$ curves (curve 6 in Fig. 3). The subsequent rise of the velocity v_+ in fields more than twice the threshold value, observed for liquids, is attributed to stochastic slip of the captured charge. This mechanism may be active also in solid helium.

4.4. Strong-field dependence of the negative-charge velocity

The problem of the motion of a negatively charged cavity or a positively charged ice particle in solid helium in the thermally activated motion range has not been investigated in strong fields. In a review of Ref. 11 it is shown that continuation of Shikin's calculations[10] for classical vacancies would give rise to terms of the type $\alpha E^3 + \beta E^5$, similar to the expansion as a series of Eq. (3), which can be rewritten as follows:

$$v_-(T, E) = \mu_- E (kT/eEb) \operatorname{sh}(eEb/kT). \qquad (3a)$$

The average values of the parameter b calculated using all the experimental points are almost an order of magnitude less than the interatomic spacing. This may be because the volume of a negatively charged cavity is much less than the volume per atom in the lattice, and one elementary event (absorption and emission of a vacancy, motion of an atom on the internal surface) can shift a charge as a whole along the field E by a distance less than the atomic spacing.

At temperatures above 1 K the field dependences of the velocity of positive charges in samples of the type shown in Fig. 4a are similar to the field dependence of the negative charge velocity. The dependences (3) and (3a) can be used to describe also the results of measurements of the velocity of charges in bcc ^{3}He crystals[12,20] in which vacancies are known to be localized because of the presence of a nuclear spin. Moreover, it is known that the dependence of the velocity of a metallic sphere frozen into solid ^{4}He is also steeper than cubic under the influence of strong forces,[26] but the motion of a small sphere in helium is controlled by dislocations with activation energies close to ε_v (Ref. 27). Therefore, it would be desirable to carry out such measurements in the same sample in order to shed light on the mechanism of motion of test particles of different types in solid helium subjected to strong fields.

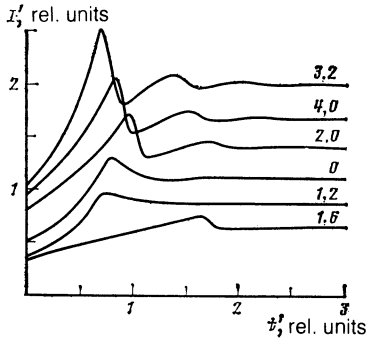

FIG. 12. Model dependence $v^*(E)$ represented by the continuous curve compared with the results of a calculation of the average velocity of a front in a diode (○) and of the steady-state current (●) observed for a given voltage U.

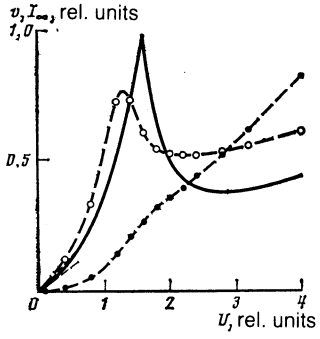

FIG. 13. Time dependence of the collector current observed on application of a voltage step U (the numbers are alongside the curves). The initial dependence $v^*(E)$ is the same as in Fig. 12.

5. CONCLUSIONS

Extending the range of measurements of the velocity of injected charges in hcp ^{4}He crystals and comparing the results obtained with theory demonstrated that the existing theoretical models cannot satisfactorily describe the accumulated data. It is necessary to carry out further theoretical investigations of the transport of a charged defect in nonregular quantum crystals allowing not only for the structure of charges in helium, but also for the crystal structure of the samples.

The authors are grateful to A. V. Lokhov and V. N. Khlopinskiĭ for their help in setting up the experiments, and also to participants of an All-Union Colloquium on Quantum Liquids and Crystals (Bakuriani, 1986) for valuable discussions.

APPENDIX

Figures 12 and 13 show the results of a numerical calculation of the time dependence of the charge velocity and of the collector current in the case of a planar diode with a source of infinite power (so that the collector current is limited by the space charge) in the case of a given nonmonotonic model dependence of the velocity of a single charge v^* on the field E. The system of model equations was the same as that used in Refs. 18 and 19.

The continuous curve in Fig. 12 is the model dependence $v^*(E)$, whereas the dashed curves $v(U)$ and $I_\infty(U)$ are drawn through the calculated values of the average velocity and the steady-state current obtained for a given value of U. The time dependence of the current $I(t)$ corresponding to a given dependence $v^*(E)$ and obtained for several values of U (values alongside the curves) near the threshold voltages is plotted in Fig. 13. For convenience, we used dimensionless units:

$$I' = IL^2/\varepsilon_0 U v^* S, \quad t' = tv^*/L,$$

i.e., time is normalized to the time taken to cross the source–collector base by a single charge in a field $E = U/L$; S is the collector area. The number 0 in Fig. 13 represents the $v(U)$ curve in the limit of weak fields, where $v^* \propto E$. This curve is identical with those calculated in Refs. 18 and 19. The shape of the curves changes as the voltage increased, as indeed found in the experiments (Fig. 6). The arrival of a charge

front at a collector corresponds to the position of the first maximum of the $I(t)$ curves.

It is clear from Fig. 12 that the $v(U)$ curve repeats qualitatively the dependence $v^*(E)$, although the amplitude and position of the maximum are quite different for each of the curves. In contrast to the average velocity, the steady-state current I_∞ through a collector rises with the field experiencing only a slight inflection in fields near the threshold (and the experimental curve in Fig. 5 behaves similarly).

[1]A. I. Shal'nikov, Zh. Eksp. Teor. Fiz. **41**, 1059 (1961) [Sov. Phys. JETP **14**, 755 (1962)]; **47**, 1727 (1964) [**20**, 1161 (1965)].
[2]E. Ifft, L. P. Mezhov-Deglin, and A. I. Shal'nikov, Proc. Tenth Intern. Conf. on Low Temperature Physics, Moscow, 1966, Vol. I, VINITI, Moscow (1967), p. 224.
[3]K. O. Keshishev, Yu. Z. Kovdrya, L. P. Mezhov-Deglin, and A. I. Shal'nikov, Pis'ma Zh. Eksp. Teor. Fiz. **10**, 427 (1969) [JETP Lett. **10**, 274 (1969)].
[4]K. O. Keshishev, L. P. Mezhov-Deglin, and A. I. Shal'nikov, Pis'ma Zh. Eksp. Teor. Fiz. **12**, 234 (1970) [JETP Lett. **12**, 160 (1970)].
[5]K. O. Keshishev, L. P. Mezhov-Deglin, and A. I. Shal'nikov, Proc. Twelfth Intern. Conf. on Low Temperature Physics, Kyoto, Japan, 1970, Academic Press of Japan, Tokyo (1971), p. 141.
[6]K. O. Keshishev and A. I. Shal'nikov, Fiz. Nizk. Temp. **1**, 590 (1975) [Sov. J. Low. Temp. Phys. **1**, 285 (1975)].
[7]K. O. Keshishev, Zh. Eksp. Teor. Fiz. **72**, 521 (1977) [Sov. Phys. JETP **45**, 273 (1977)].
[8]K. O. Keshishev and A. É. Meĭerovich, Zh. Eksp. Teor. Fiz. **72**, 1953 (1977) [Sov. Phys. JETP **45**, 1027 (1977)].
[9]A. F. Andreev, Usp. Fiz. Nauk **118**, 251 (1976) [Sov. Phys. Usp. **19**, 137 (1976)].
[10]V. B. Shikin, Usp. Fiz. Nauk **121**, 457 (1977) [Sov. Phys. Usp. **20**, 226 (1977)].
[11]A J. Dahm, in Progress in Low Temperature Physics (Ed. D. F. Brewer), Vol. 10, p. 73 (North–Holland, Amsterdam, 1985).
[12]V. B. Efimov and L. P. Mezhov-Deglin, Fiz. Nizk. Temp. **4**, 397, 857 (1978) [Sov. J. Low. Temp. Phys. **4**, 195, 406 (1978)].
[13]L. P. Mezhov-Deglin, V. B. Efimov, and A. I. Golov, Fiz. Nizk. Temp. **10**, 99 (1984) [Sov. J. Low. Temp. Phys. **10**, 53 (1984)].
[14]A. I. Golov, V. B. Efimov, and L. P. Mezhov-Deglin, Pis'ma Zh. Eksp. Teor. Fiz. **38**, 58 (1983) [JETP Lett. **38**, 65 (1983)].
[15]A. I. Golov, V. B. Efimov, and L. P. Mezhov-Deglin, Pis'ma Zh. Eksp. Teor. Fiz. **40**, 293 (1984) [JETP Lett. **40**, 1080 (1984)].
[16]L. G. Gross and N. N. Gabitova, Izot. SSSR No. 27, 32 (1972).
[17]M. A. Lampert and P. Mark, *Current Injection in Solids*, Academic Press, New York (1970).
[18]A. V. Gudenko and V. L. Tsymbalenko, Zh. Eksp. Teor. Fiz. **76**, 1399 (1979) [Sov. Phys. JETP **49**, 712 (1979)].
[19]A. Many and G. Rakavy, Phys. Rev. **126**, 1980 (1962).
[20]V. B. Efimov, Thesis for Candidate's Degree [in Russian], Institute of Solid State Physics, Academy of Sciences of the USSR, Chernogolovka, Moscow Province (1982), p. 125.
[21]V. A. Mikheev, N. P. Mikhin, and V. A. Maĭdanov, Fiz. Nizk. Temp. **9**, 901 (1983) [Sov. J. Low. Temp. Phys. **9**, 465 (1983)].
[22]R. O. Simmons, Invited Paper presented at Conf. on Quantum Liquids and Solids, Banff, Canada, 1986.
[23]A. F. Andreev and A. É. Meĭerovich, Zh. Eksp. Teor. Fiz. **67**, 1559 (1974) [Sov. Phys. JETP **40**, 776 (1975)].
[24]Yu. Kagan and L. A. Maksimov, Zh. Eksp. Teor. Fiz. **84**, 792 (1983) [Sov. Phys. JETP **57**, 459 (1983)].
[25]L. H. Nosanow and W. J. Titus, J. Low Temp. Phys. **1**, 73 (1969).
[26]H. Suzuki, J. Phys. Soc. Jpn. **35**, 1472 (1973).
[27]A. A. Levchenko and L. P. Mezhov-Deglin, Zh. Eksp. Teor. Fiz. **86**, 2123 (1984) [Sov. Phys. JETP **59**, 1234 (1984)].

Translated by A. Tybulewicz